Mon. Not. R. astr. Soc. (1981) **195**, 939–957

Chemical compositions of H II regions in the Triangulum spiral, M33

Karen B. Kwitter* and Lawrence H. Aller
Astronomy Department, University of California, Los Angeles, California 90024, USA

Received 1980 October 21; in original form 1980 July 30

Summary. Measurements of 12 H II regions secured with the Robinson–Wampler Image Tube Scanner at the Shane Telescope, Lick Observatory cover the spectral range λλ 3700–7600. The distances of these regions from the nucleus range from 1 to 6 kpc. These data are analysed to establish plasma diagnostics and chemical compositions. In a manner similar to that previously employed for studies of the Magellanic Clouds, theoretical models are used as interpolation devices to establish ionization correction factors for S, Cl and Ar. Except for helium, the N(element)/N(H) ratios fall off with increasing radial distance with closely similar rates. Consequently, the ratios not only of nitrogen, but also neon, sulphur and argon, with respect to oxygen, remain essentially constant. The following log N(element)/N(oxygen) are found: N = −1.25, Ne = −0.77, S = −1.5, Cl = −3.6 and Ar = −2.4.

Introduction

The Triangulum galaxy is the nearest Sc spiral. It has been classified as Sc (Hubble 1936) and ScII–III (van den Bergh 1960). It has well developed spiral arms although the nucleus NGC 598 is very inconspicuous and, as galactic nuclei go, very quiet. Israel & van der Kruit (1974) found no radio-frequency source at the optical centre to their limit of 1.2 milliflux units (mfu). For comparison, if Sgr A were there, it would be a point source with a flux of 80 mfu. Walker (1964) found a distinct nucleus with a diameter of 1 to 1.4 arcsec. Mayall & Aller (1942) found an absorption spectrum resembling A7; the [O II] λ 3727 emission may come from surrounding gas. Although the nucleus of our Galaxy has been likened to an accumulation of star clusters, that of a galaxy such as M33 may be dominated by individual stars (van den Bergh 1976). Gordon (1969) has summarized the early history of work on M33.

H II regions

Early lists of emission nebulosities were prepared from examination of direct photographs (see, e.g. Mayall & Aller 1939, 1942) but with the advent of fast red-sensitive emulsions and

* Present address: Hopkins Observatory, Williams College, Williamstown, Massachusetts 01267, USA.

Some basic data for M33

Position angle of major axis	20° [1]; 22° ± 1° [2]
Inclination	57° [1]; 54° ± 3° [2]
Systemic radial velocity	− 172 km s^{-1} [1]; − 180 [2]
Distance	720 kpc [3]
Mass ($10^{10} M_{\odot}$)	1.29 [4]; 0.92 [2]
Mass-to-light ratio	4.9 ± 0.3 [2]
Neutral hydrogen	Pattern similar to optical with density decreasing from 1 cm^{-3} to 0.4 cm^{-3} at 5 kpc [5]

[1] Mayall & Aller (1942).
[2] Warner, Wright & Baldwin (1973).
[3] Sandage (1962), van der Kruit (1973), de Vaucouleurs (1978).
[4] Lohmann (1974).
[5] Wright *et al.* (1972).

relatively narrow band-pass filters it was possible to find and measure many more objects (Haro 1950; Aller 1950, 1954, 1956; Shajn 1954; Sandage 1962; Hodge 1969). Finally, with the development of fast optical systems and interference filters it was possible to detect very faint H II regions, interarm gas, etc. (see, e.g. Courtes & Cruvellier 1965). So far, the most complete catalogue is that given by Boulesteix *et al.* (1974), based on observations obtained with a focal reducer and narrow bandpass filter (~ 25 Å at Hα). In addition to discrete H II regions, they note an extensive background emission that connects H II regions in the arms. Although H I and H II spiral structure are strongly correlated, most of the H II regions in M33 appear not in the densest parts of the H I clouds, but on the edges thereof. In fact, the most intense H II regions such as NGC 588, 592, 595, 604 and IC 131 are found outside the spiral arms. Presumably, star formation occurs not where the density is greatest, but rather where the *density gradient* is greatest.

With the Westerbork synthesis telescope, Israel & van den Kruit (1974) measured sources down to 1.2 mfu at 1415 MHz. They obtained a resolution of 23 × 45 arcsec (78 × 158 pc). At the distance of M33, Orion would have a flux of 0.25 mfu. Hence, according to Mezger's (1970) definition, all H II regions so far observed in Messier 33 are giant H II regions.

Since the apparent diameter of the individual H II regions they observed increased with exposure time, Boulesteix *et al.* (1974) concluded that most H II regions are density bounded, as did Comte & Monnet (1974) who argued that the interarm region is ionized by radiation from hot stars in spiral arms. From their radio data, Israel & van der Kruit (1974) drew a different conclusion. If you plot electron density against diameter, all nebulae fall above the excitation parameter $u = 115$ which corresponds to the detection limit of the system; but $u = 210$ defines an upper limit to the observed excitation parameter. Thus, a maximum UV photon production rate exists, irrespective of other factors such as diameter or $\langle N_e^2 \rangle$ and they conclude that H II regions in M33 are ionization bounded or photon limited.

Spectroscopic and abundance studies

An early spectroscopic study of 19 emission regions in M33 (Aller 1942) was restricted to the λλ 5007–3727 region. Calibrated eye estimates of intensities gave estimates of [O III]/Hβ, [O II]/Hβ and revealed a dependence of the [O III]/[O II] ratio on distance from the nucleus, which was then interpreted as an excitation rather than an abundance effect. Searle (1971)

made photoelectric measurements of the absolute brightness in Hα, Hβ, [O II], [O III] and [N II] for eight bright H II regions and measured the Hβ/[O II] ratio in 24 additional objects. He favoured the hypothesis that the change in appearance of the spectrum was largely due to a composition gradient. Smith (1975) investigated several emission regions and determined the electron temperature in outer regions of the spiral. He concluded that in M33 as in M101 there is a strong radial gradient in the O/H ratio, apparently a weak N/O ratio variation, and constant Ne/O and S/O ratios.

Other observers (Benvenuti, D'Odorico & Peimbert 1973; Comte 1975; Comte & Monnet 1974) have studied intensity variations of Hα, [N II] and [S II] as a function of distance from the centre of M33.

From monochromatic photographs in [O I] radiation, Comte found no H II regions, although [O III] photographs showed many H II regions. Thus, the [O I] lines recorded on spectra of H II regions may originate in strata well removed from H II regions.

The great strength of [S II] presents some difficulties. It is often observed that the [S II]/Hα ratio increases significantly toward the centres of galaxies (Peimbert 1971; Warner 1973; Rubin & Ford 1971). In M33 it is noted that the fainter the H II region, the larger the [S II]/Hα ratio.

Peimbert, Rodriguez & Torres-Peimbert (1974) have discussed the difficulties posed by the behaviour of the [S II] lines in M33 and similar H II regions in other galaxies.

Our own theoretical models can predict [S II] intensities agreeing with those observed for ionization-limited models, i.e. full Strömgren spheres, but *not* for material-limited models (truncated Strömgren spheres). Composite or segmented models (leaky Strömgren spheres) can yield [S II] lines of moderate intensity and provide radiation to ionize the surrounding medium. It seems possible that such inhomogeneous structures can reconcile the seemingly conflicting data of Boulesteix *et al.* (1974) on the one hand and Israel & van der Kruit (1974) on the other.

Although S^+ can exist in H^0 regions, it seems unlikely that much [S II] radiation can originate there because the electron density must be very low. Most of the [S II] radiation must come from the N^+, O^+, H^+ zone, i.e. from at least low-excitation H II zones.

Strong [S II] radiation is a popular discriminant for supernova remnants, where the radiation is produced behind the shock front. Three supernova remnants have been identified in M33 by Danziger *et al.* (1979). Dopita, D'Odorico & Benvenuti (1980) have compared spectroscopically a number of supernova remnants and H II regions in M33 in a program to find absolute abundance gradients. It seems unlikely that [S II] enhancements in ordinary H II regions are to be attributed to shock phenomena.

Thus M33 is a spiral system with a rich gaseous component and numerous early-type stars although, per unit mass, there are possibly fewer such objects than in our galactic system (Israel & van der Kruit 1974). H II regions are fundamental to assessing the chemical composition of the interstellar medium and establishing clues to the early history of chemical processing. The H II regions involved here are all giant structures indicative of active domains of recent star formation. They are excited by several early O-type stars. Chemical composition of the interstellar medium, data on stellar content, mass distribution, and distribution of H^0 will all assist in working out the history of this galactic chemical evolution.

Observational programme

Our objectives were to (a) cover the spectra of H II regions in the 3700–8000 Å interval as thoroughly as practical, choosing objects distributed in distance from about 1 kpc from the nucleus out to nearly 30 arcmin or about 6 kpc away; (b) observe the diagnostic ratios

[O III] 4959 + 5007/4363, [S II] 6717/6731, [O II] 3727/7325 and [N II] 6584/5755 for NGC 604 (the chlorine lines 5517/5537 are too weak to supply a satisfactory ratio for diagnostic needs); (c) improve the abundances and abundance gradients of He, N, O and Ne and also S and Ar (plus Cl in MA3 and NGC 604).

All of the observations were secured with the Robinson–Wampler (1972) Image Dissector Scanner. In the newer more versatile version of the instrument, slot sizes, wavelength settings and gratings could be changed easily. One observes the object alternately in the left and right slot usually with a dwell time of 4 min in each position.

We employed a 2 x 2 arcsec slot size. We summed the scans, subtracted the sky, applied flat-field corrections, corrected for atmospheric extinction, and linearized the wavelength scales of the resultant scans by standard techniques. Appropriate observations of a standard star chosen from a list by Stone (1974) enables us to derive the response function and reduce the scans to fluxes expressed in cgs units.

Intensities of individual lines may be measured by a machine program or directly by eye from the plots. We often preferrred the latter procedure because of noise in the scans. In each method the continuum position is judged by eye. For weak lines in a noisy scan the error may exceed 50 per cent. Areas of strong lines were found to be repeatable to 7 per cent. We combine line intensities from different grating settings by using strong lines in the overlap region.

Overlapping profiles such as λλ 6548, 6584 [N II] and Hα can be deconvolved by a straightforward procedure – since the instrumental profile is known.

Sources of error may be summarized briefly as follows: the strong, essentially stellar background continuum introduces errors through random photon statistics. Placement of this continuum can be difficult and can lead to systematic errors that are especially severe for weak lines. Except where otherwise noted, we believe the error in 5007/4363 to amount to 20–30 per cent. In IC131, the intensity of λ 4363 may have been overestimated by a factor of 2.

Interstellar extinction can be assessed by comparing observed Balmer line intensities with the theoretical 'case B' decrement (Clarke 1965; Brocklehurst 1971). We assumed the Whitford (1958) reddening function and obtained the logarithmic correction $C(H\beta)$.

By comparing Searle's Hβ fluxes with their own 21-cm data, Israel & van der Kruit (1974) found C values greater by 0.4 to 0.8 than those reported by Searle. The discordance may arise from internal dust (*cf.* Mathis 1970).

In Figs 1–7 we reproduce some representative scans for MA3 and NGC 604. In Figs 2, 3 and 6 two or more scans are shown with different magnifications. Some H II regions show

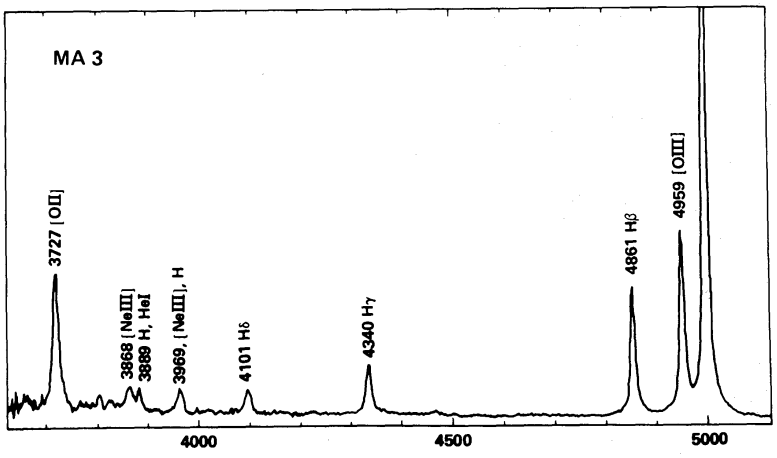

Figure 1. Scan of spectrum of MA3 (λλ 3700–5100 Å).

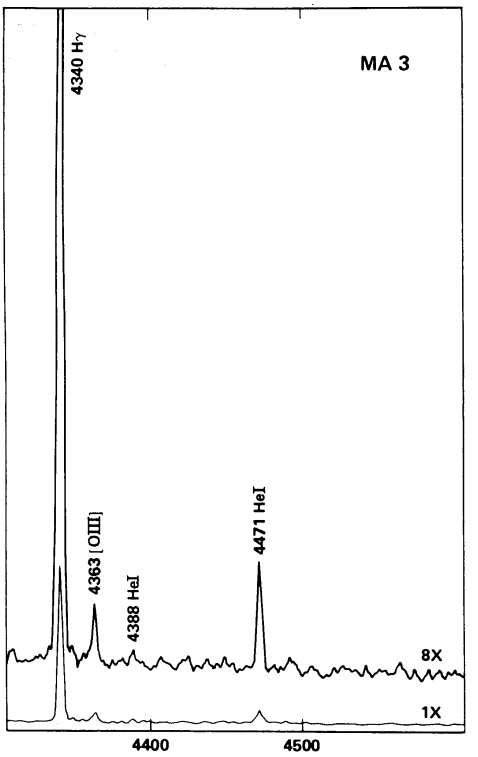

Figure 2. Higher dispersion scan of region λλ 4300–4600 Å in MA3. Here λ 4363, [O III], He I 4388 and He I 4471 are easily measurable. Two magnifications, 1× and 8×, are employed. This scan was secured with higher dispersion.

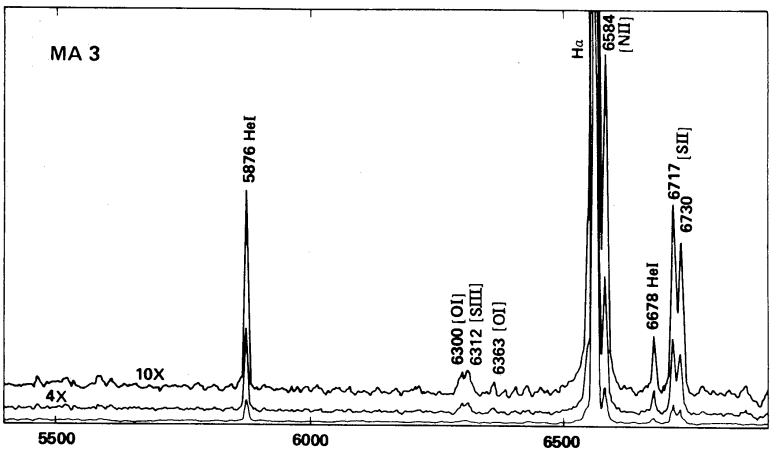

Figure 3. The region λλ 5400–6900 Å in MA3. Magnifications of 1×, 4× and 10× are displayed.

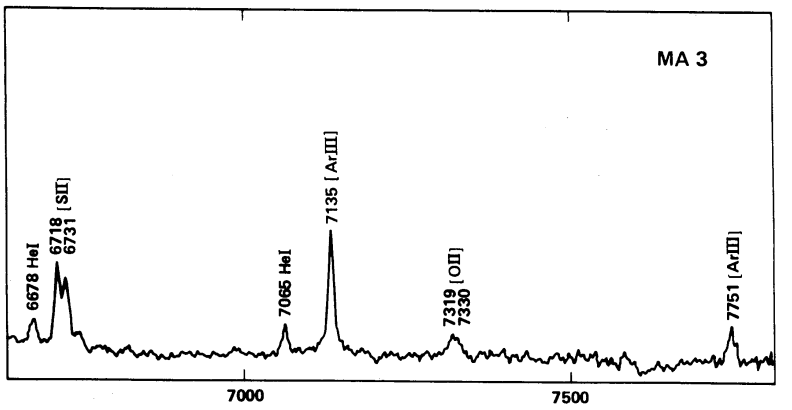

Figure 4. The deep red region λλ 6620–7800 Å of MA3 is displayed.

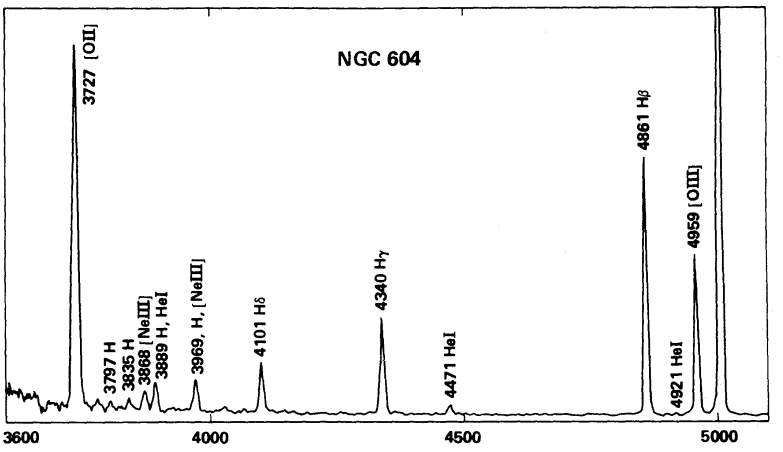

Figure 5. The spectrum of NGC 604 in the region λλ 3600–5100 Å.

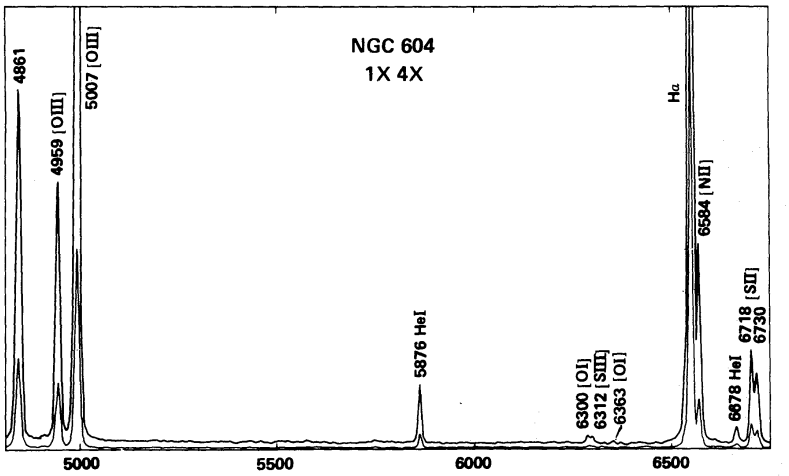

Figure 6. The spectrum of NGC 604, λλ 4820–6750 Å. Magnifications of 1× and 4× are employed.

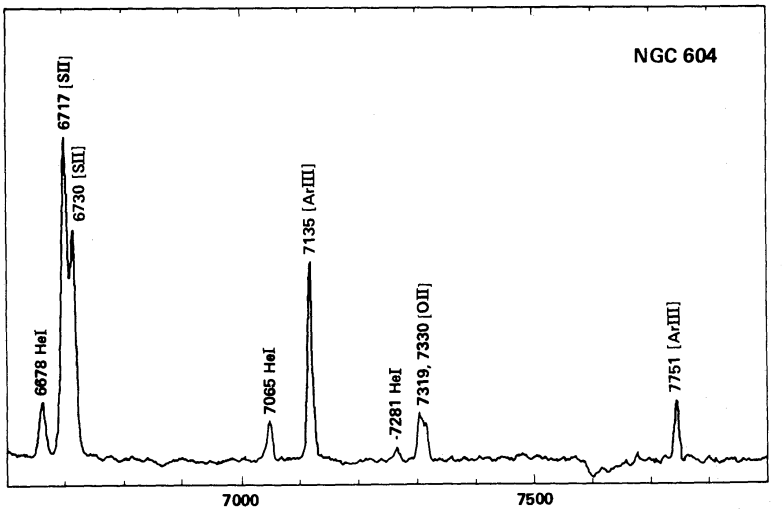

Figure 7. The spectrum of NGC 604, λλ 6600–7900 Å. Notice the prominence of [O II] λλ 7319, 7330 and He I, λλ 6678, 7065, [Ar III] λλ 7135, 7751.

Table 1. Data for observed H II regions.

Region		(1950) α	δ	r(arc min)*	r(kpc)*
MA11	85	1:31:12	30:23:45	4.7	0.98
IC142	301	1:31:12	30:30:07	6.1	1.28
NGC595	49	1:30:45	30:26:30	7.5	1.57
MA2	88	1:31:25	30:22:15	10.6	2.22
MA3		1:31:12	30:36:43	13.5	2.83
NGC604	680	1:31:43	30:32:05	14.6	3.06
IC131	290A	1:30:21	30:30:12	18.3	3.83
MA9a	650	1:31:42	30:45:12	22.6	4.73
IC133	423	1:30:25	30:38:00	23.4	4.90
NGC588	280	1:29:55	30:23:48	24.0	5.03
IC132	638	1:30:26	30:41:36	27.1	5.68
MA1		1:30:12	30:56:36	29.8	6.24

* In the plane of M33, assuming an inclination of 57° to the line of sight and a major axis position of 20°. The distances are calculated for an assumed distance of 720 kpc. D(o) = 50′ (de Vaucouleurs & de Vaucouleurs 1964). Coordinates of centre $\alpha = 01^h\,31^m\,01^s.2$; $\delta = +30°\,24'\,27''$ (1950), Warner *et al.* (1973).

Wolf–Rayet 'bands' near λ4640, which is not surprising in view of the discovery of several Wolf–Rayet stars in M33 by Wray & Corso (1972).

Table 1 lists the H II regions observed. The first column gives the designation of the object; MA denotes the number in the list by Mayall & Aller (1942). The second column gives the designation in the catalogue by Boulesteix *et al.* (1974). The third and fourth columns give (α, δ) (1950) and the last two columns the distances of the nebulosities from the nucleus. As a sample of the variations of line ratios with respect to distance from the nucleus, Fig. 8 shows the behaviour of [N II]/[S II]. The distinct decline is to be attributed to a substantial weakening of [N II] with increasing distance from the centre of the galaxy. The effect is much more marked than in Fig. 2 of Comte (1975) where $I(6584)$ is strongly affected by the OH λ6577 airglow line.

Table 2 gives the finally adopted logarithms of line intensities referred to Hβ and corrected for interstellar extinction by the Whitford (1958) curve. The last line of the table gives $C(H\beta)$.

Analysis of the data

In comparison with rich diagnostic data often available for planetary nebulae, only rather limited data are to be had for H II regions in M33. $[I(4959) + I(5007)]/I(4363)$ ratios have

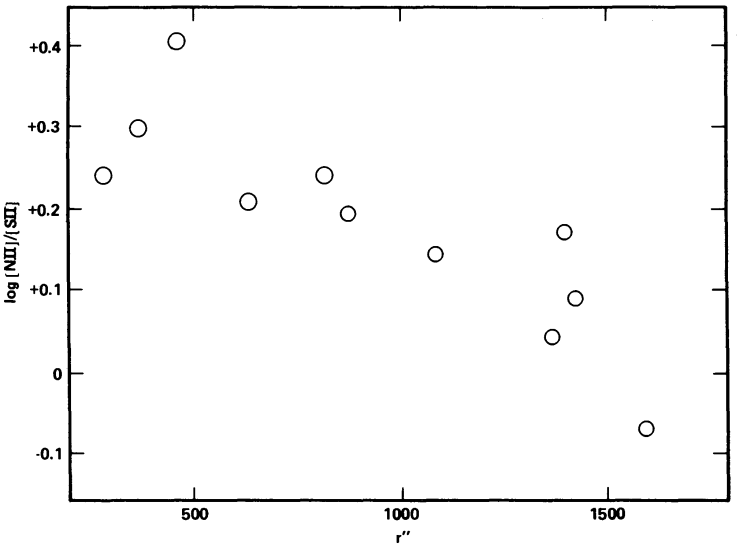

Figure 8. Dependence of the [N II]/[S II] ratio on distance from centre of nebula. [N II] λλ 6548, 6584 appear to weaken more steeply with distance than do the [S II] lines.

been measured only for NGC 604, IC131, NGC 588 and IC132. For several additional nebulosities, NGC 595, MA3 and IC133, we have corroborative evidence from the 3727/7325 ratio. This ratio depends on both N_ϵ and uncertainties in the interstellar extinction, and hence is inferior to 5007/4363 as a temperature discriminant. The electron density sensitive 6730/6717 [S II] ratio is available for all our objects. For most objects $N_\epsilon \leqslant 200$ cm^{-3}. Columns (2) and (3) of Table 3 list the adopted values of $\log x$ and t where $x = 10^{-4}\, T_\epsilon/\sqrt{N_\epsilon}$ and $t = [T_\epsilon/10\,000]$. Values of the temperature indicated in parentheses are adopted from considerations of theoretical models.

The remaining columns of Table 3 give ionic concentrations calculated by conventional expressions for the appropriate forbidden lines. We use [N II], [O III] and [Ne III] data from Seaton (1975), and [S II] data from Pradhan (1978). For [S III], [Cl III] and [Ar III] we have used cross-section data by Krueger & Czyzak (1970). The A-values are basically those compiled by Garstang (1968), updated when necessary by more recent data (Nussbaumer 1971; Osterbrock 1974). Accurate, modern expressions for deriving T_ϵ from [O III] and [N II] are given by Seaton (1975). We append notes for individual objects discussed in this investigation.

In our derivation of ionic concentrations for nebulosities for which no direct measurement of T_ϵ via the $[N_1 + N_2]/4363$ ratio or estimate from 3727/7325 is at hand, we have to use an indirect argument. Shields & Searle (1978) proposed a theoretically sound procedure for calculating the stellar flux and nebular ionization structure and, thus, estimating T_ϵ. Unfortunately, its application requires data that we do not have. In the interior regions of M101, where the metal/H ratio exceeds the solar value, they were able to show that T_ϵ was much lower than in H II regions where the diagnostic lines are normally observed.

It has long been known that when the concentration of atoms such as oxygen is increased in a plasma exposed to a fixed field of radiation, the electron temperature is lowered (Menzel & Aller 1941). This basic relationship has been employed by Pagel *et al.* (1979) and by Alloin *et al.* (1979) to derive electron temperatures and elemental abundances in objects where λ 4363 is not observed. Pagel *et al.* (1979) use ([O II] + [O III])/Hβ as a fundamental parameter, combined data for several galaxies, and give plots of $\log n(O)/n(H)$ and T_ϵ against this parameter. They find an increase of [O II] + [O III]/Hβ from 2.5 to

Table 2. Line intensities [log $I/I(H\beta)$].

λ	Ident.	MA11	IC142	NGC595	MA2	MA3	NGC604	IC131	MA9a	IC133	NGC588	IC132	MA1
3727	[OII]	0.50	0.44	0.46	0.06	0.24	0.42	0.30	0.55	0.16	-0.06	0.03	
3770	H		-1.50:	-1.50:			-1.27						
3797	H		-1.39	-1.51:			-1.53						
3835	H		-1.38	-1.46:			-1.32				-2.00	-1.40	
3869	[NeIII]		-1.70	-1.02		-0.71	-1.04	-1.17	-0.67	-0.49	-0.36	-0.33	
3889	H,He	-0.71	-0.88	-0.89	-0.75	-0.92	-0.88	-0.84		-0.68	-0.79	-0.79	
3968/70	[NeIII],He	-0.86	-0.95	-0.97		-0.60	-0.77	-0.77		-0.65	-0.71	-0.65	
4026	HeI						-1.43						
4068/76	[SII]		-1.40				-1.73						
4101	Hδ	-0.44	-0.87	-0.67	-0.72	-0.72	-0.58	-0.70	-0.69	-0.65	-0.74	-0.64	
4340	Hγ	-0.37	-0.32	-0.41	-0.51	-0.34	-0.34	-0.43	-0.33	-0.33	-0.33	-0.33	-0.48:
4363	[OIII]					-1.66	-1.74	-1.65:			-1.10	-1.14	
4471	HeI	-1.28	-1.53	-1.47:		-1.45	-1.42				-1.37		
4861	Hβ	0.00	0.00	0.00	0.00	0.00	0.00	0.00	0.00	0.00	0.00	0.00	0.00
4921	HeI		-2.32			-1.93	-2.33				-1.68		
4959	[OIII]	-0.61	-0.51	-0.28	-0.19	0.19	-0.17	-0.15	-0.20	0.25	0.28	0.29	0.27:
5007	[OIII]	-0.15	-0.01	0.18	0.29	0.62	0.32	0.33	0.23	0.72	0.75	0.75	0.76:
5517/37	[ClIII]					-2.05	-2.23						
5755	[NII]						-2.48						
5876	HeI	-1.11	-1.10	-1.08	-0.90	-0.95	-1.09	-0.99	-0.86	-1.00	-0.92	-0.88	
6300	[OI]		-1.86	-1.86	}	-1.72	-1.98			-1.68			-0.22:
6312	[SIII]		-2.24	-1.76			-2.01			-1.87			-0.22:
6363	[OI]		-2.39				-2.30						
6548	[NII]	-0.75	-0.72	-0.88	-1.34	-1.24	-1.03	-1.15	-0.94	-1.42	-1.55	-1.63	
6563	Hα	0.45	0.45	0.45	0.45	0.45	-0.45	0.45	0.45	0.46	0.45	0.45	0.45
6584	[NII]	-0.37	-0.28	-0.42	-0.86	-0.77	-0.55	-0.78	-0.47	-0.94	-1.07	-1.15	
6678	HeI	-1.44	-1.49	-1.50	-1.52	-1.58	-1.56	-1.42	-1.11	-1.59	-1.59	-1.17	
6717	[SII]	-0.68	-0.68	-0.93	-1.16	-1.13	-0.82	-1.00	-0.64	-1.17	-1.28	-1.19	-0.15:
6731	[SII]	-0.84	-0.84	-1.09	-1.36	-1.24	-1.00	-1.14	-0.75	-1.38	-1.36	-1.29	-0.15:
7065	HeI			-1.84		-1.71	-1.83	-1.65		-1.75			
7135	[ArIII]	-1.30		-1.11		-1.08	-1.12	-1.11		-1.01	-1.26	-1.16	
7321	[OII]			-1.28		-1.57	-1.50	-1.75		-1.51			
7751	[ArIII]					-1.64	-1.77			-1.46			
C(Hβ)		0.70	0.70	0.68	0.25	0.55	0.38	0.47	0.11	0.57	0.30	0.60	0.30:

: Denotes an uncertain value

Table 3. Ionic concentrations log $N(i)/N(H)$.

	Log x	t	He^+	N^+	O^+	O^{++}	Ne^{++}	S^+	S^{++}	Ar^{++}
MA11	-2.5	(0.8)	10.97	7.18	8.53	7.73	-	6.13	-	5.85
IC142	-2.0	(0.8)	10.76	7.28	8.47	7.87	6.72	6.08	6.59	
NGC595	-2.0	0.9	10.81	6.98	8.17	7.81	7.16	5.74	6.82	5.90
MA2	-2.5	(0.8)	10.95	6.70	7.97	8.17		5.63		
MA3	-1.7	0.93	10.88	6.59	7.95	8.26	7.41	5.51	<6.6	5.90
NGC604	-2.3	1.08	10.89	6.87	8.22	7.73	6.82	5.82	6.58	5.71
IC131	-2.0	1.15	10.89	6.34	7.63	7.65	6.60	5.41		5.66
MA9a	-1.65	(1.0)	11.01	6.81	8.11	7.75	7.21	5.92		
IC133	-2.5	1.1	10.88	6.23	7.56	8.10	7.34	5.25		5.80
NGC588	-1.5	1.28	10.96	5.95	7.10	7.94	7.24	5.07		5.42
IC132	-1.6	1.23	11.00	5.91	7.24	7.99	7.33	5.15		5.55
MA1	(-2)	1.0				7.27				

10.0 to correspond to a *decrease* in the oxygen abundance $n(O)/n(H)$ by an order of magnitude. The explanation of this paradoxical result is that the decrease in cooling and consequent rise in T_e more than compensates for the fewer ions present. Over the same range T_e rises from about 6000 to about 12 000 K. A similar effect seems to exist in our own Galaxy (Churchwell *et al.* 1978; Wilson 1979; Mezger *et al.* 1979).

For the inner H II regions in M33, we adopted T_e = 8000 K as a reasonable upper limit, on the basis of data by Pagel *et al.* (1979).

Extrapolation from ionic concentrations to abundances may be made by formulae such as those proposed by Peimbert & Costero (1969) and employed by many others. Model nebular calculations (Hawley & Grandi 1978; Aller, Keyes & Czyzak 1979) suggest that the approximation for nitrogen is reasonable for low to medium excitation nebulae. Plausible values are found for neon, although model calculations often predict a higher Ne/O ratio.

Another approach is to use theoretical models (Balick & Sneden 1976; Stasinska 1978, 1979; Sarazin 1976; Aller *et al.* 1979). The models employed here are based on a formulation that is due to Balick (1975). Our procedure, described by Keyes & Aller (1978), allows the calculation of composite models and has been modified to include recent data on charge

exchange reactions (Butler, Bender & Dalgarno 1979). We employed the models as interpolation devices for estimating ionization correction factors (ICF) for helium, sulphur, chlorine and argon. Charge exchange effects appear to be important. Uncertainties in the relevant cross-sections can produce large effects on the ionization equilibrium.

We calculated an extended network based on Kurucz's (1979) solar composition model atmospheres for T_ϵ = 30 000, 35 000, 40 000, 45 000 and 50 000 K ($\log g = 4.5$). Unfortunately, atmospheric models for different metal/H with desirable $T_{\rm eff}$ and $\log g$ values are not available. The present discussion is based on the grid summarized in Table 4. The assumed chemical composition of the nebular gas is listed at the bottom of the table. We have also calculated more limited grids for models corresponding to compositions derived in Table 5 for NGC 604, IC 132 and IC 142. Table 4 lists predicted values of $I(5876)$, $I(4959 + 5007)/3727$, $I(3727)$ and $I(5007)$ on the scale $I(\mathrm{H}\beta) = 100$. The average T_ϵ, $\langle T_\epsilon \rangle$ is given in the next to the last line and reflects the interplay between energy distributions and coolants with change of radiation field and density. The last row gives the relative size of the Strömgren sphere expressed in units of the size of the ($N_{\rm H} = 100$, $T_\epsilon = 45\,000$) model. Given a value of N_ϵ from the [S II] ratio and 3727/7325 (if available), we use the observed $[N_1 + N_2]/3727$ ratio to select (or interpolate) a model of appropriate excitation whereby ionization

Table 4. Synopsis of some model calculations.

		I(Hβ) = 100				
		30 000	35 000	40 000	45 000	50 000
$N_{\rm H}$=30	$N_1+N_2/3727$	3.5(-5)	.0152	0.89	3.6	6.1
	5876	0.68	3.7	13.3	13.5	13.4
	6584	113	149	78.1	35	30
	3727	311	520	452	281	225
	5007	.008	5.9	300	750	1026
	$\langle T_\epsilon \rangle$	8373	9316	10600	9321	9922
	R	0.306	.815	1.445	2.24	2.261
$N_{\rm H}$=100	$N_1+N_2/3727$	5.4(-5)	.023	1.32	5.5	9.1
	5876	0.68	3.66	13.4	13.5	13.3
	6584	115	149	61	24	21.6
	3727	320	520	376	203	164
	5007	.013	8.9	371	836	1110
	$\langle T_\epsilon \rangle$	8439	9356	8523	9503	10134
	R	.137	.361	.645	1.00	1.00
$N_{\rm H}$=300	$N_1+N_2/3727$	8.3(-5)	.033	1.98	8.23	13.2
	5876	.67	3.65	13.4	13.4	13.3
	6584	118	149	47	17.7	16.1
	3727	325	517	301	150	121
	5007	.020	12.8	453	923	1193
	$\langle T_\epsilon \rangle$	8546	9440	8743	9776	10429
	R	.066	.175	.308	.480	.482

Assumed Composition for Network of Models

He	0.098	Ne	8.71 (-5)
C	4.27 (-4)	S	5.01 (-6)
N	4.17 (-5)	Cℓ	1.15 (-7)
O	3.47 (-4)	Ar	1.82 (-6)

Table 5. Derived abundances for Messier 33.

Object	t	He	N	O	Ne	S	Cℓ	Ar
MA11	0.8	11.00	7.25	8.60		7.11		6.08
IC142	0.8	10.98	7.39	8.57	7.42	6.78		
NGC595	0.9	10.95	7.11	8.32	7.75	7.01		6.05
MA2	0.8	11.01	7.11	8.38		6.78		
MA3	0.93	10.95	7.10	8.45	7.63	6.75	5.02	5.94
NGC604	(*)	11.00	6.97	8.30	7.49	6.70	4.66	5.75
IC131	1.15	10.95	6.65	7.94	7.07:	6.52		5.70
	(1.0)	10.96	6.80	8.16	7.12	6.67		5.83
MA9a	(1.0)	11.16	6.97	8.28	7.33	7.10		
IC133	1.1	10.89	6.88	8.21	7.45	6.8:		5.88
	1.0	10.89	6.96	8.36	7.65	6.9:		5.97
NGC588	1.28	10.97	6.84	8.00	7.30	6.68		5.58
IC132	1.23	11.01	6.72	8.06	7.39	6.70		5.70

(*) For NGC604, we assumed t = 1.08 in hotter zones, 0.89 in cooler.

correction factors can be estimated. Note that we have also used full Strömgren spheres, i.e. ionization-limited structures. Material-limited models tend to predict [S II] intensities that are much too low.

Table 5 gives the finally calculated abundances. The models support our conclusion that $N(\mathrm{O})/N(\mathrm{H}) = [N(\mathrm{O}^+) + N(\mathrm{O}^{2+})]N(\mathrm{H}^+)$. The nitrogen and neon abundances are calculated from the aforementioned relations,

$$\frac{N(\mathrm{N})}{N(\mathrm{O})} = \frac{N(\mathrm{N}^+)}{N(\mathrm{O}^+)}$$

and

$$\frac{N(\mathrm{Ne})}{N(\mathrm{O})} = \frac{N(\mathrm{Ne}^{2+})}{N(\mathrm{O}^{2+})}.$$

We have also estimated ICFs for neon from theoretical models and have noted that they often exceed simple extrapolations. The excitation level for most H II regions is such that sulphur exists mostly as S^+ and S^{2+}. When both [S II] and λ6312 [S III] are observed, the chief source of uncertainty accrues from the measured intensity of the λ6312 line and the accuracy of $T_e(S^{2+})$. When only [S II] is observed we have to rely on model interpolation and the ionization correction factor can become large and uncertain. We have the further problem that [S II] is probably produced in low-ionization enclaves which are inadequately

handled by our models. The importance of observing λ 9069 [S III] cannot be over-emphasized (Hawley & Grandi 1977). A serious source of difficulty is that there can be excitation differences between various areas in a nebulosity. A striking illustration is found in NGC 604 where we appear to have observed an area of much lower excitation than that measured by Hawley & Grandi (1977) (compare our Table 2 and Figs 6 and 7 with their Table 1).

In the nebulae in which [Ar III] is observed, most of the atoms appear as Ar^{2+} ions; the models suggest ICF factors ranging from 1.1 to 1.4 for most objects. We suggest that when comparisons are made between gradients of elements such as N or O, which are affected by processing in the carbon cycle, and heavy elements which are produced only in advanced states of a star's evolution, we choose Ar rather than S. In objects of moderate to high excitation the relevant lines all fall in observable spectral regions. Chlorine is observed only as [Cl III]. From the models we infer an ionization correction factor of abour 1.4 for both NGC 604 and MA3.

Helium presents a difficult problem. Our models suggest much smaller correction factors than those indicated by the calculations by Peimbert *et al.* (1974). Indeed, Stasinska's (1979) investigations illustrate that inhomogeneities inflict large uncertainties on helium abundance determinations.

Discussion

The principal results of the investigation are summarized in Table 5; some further correlations are shown in Figs 9 and 10. In Fig. 9, we plot $\log N(O)/N(H) + 12$ versus distance from the nucleus. Note the systematic decline in the oxygen abundance with distance from the centre. Compare Searle (1971), Smith (1975) and Pagel *et al.* (1979). The corresponding

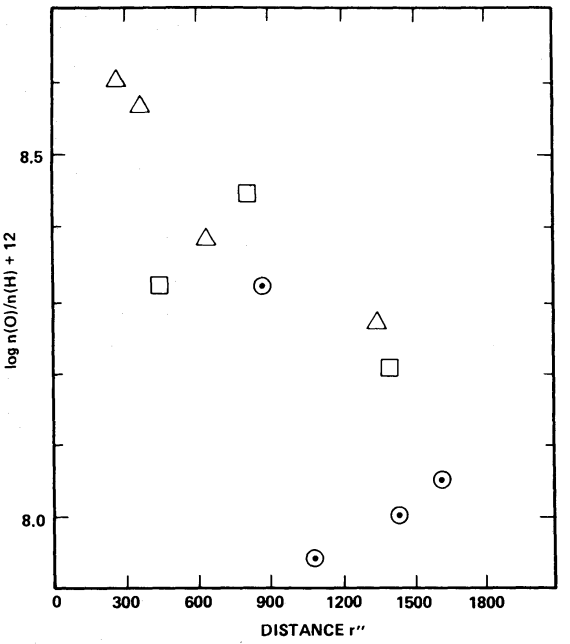

Figure 9. The $N(O)/N(H)$ gradient in M33. Note the steady decline in abundance with distance from nucleus in agreement with results found by various investigators (see text). The low point corresponds to IC 131 with an assumed temperature of 11 500 K. If we assume $T_e = 10\,000$ K, the discordance is largely removed. Δ: T_e is assumed to be 8000 K for MA11, IC142, MA2 and 10 000 K for MA9a. □: T_e from 3727/7325 [O II] ratio and limits on x. ⊙: T_e from $[I(4959) + (5007)]/I(4363)$ ratio. Compare with Pagel *et al.* (1979).

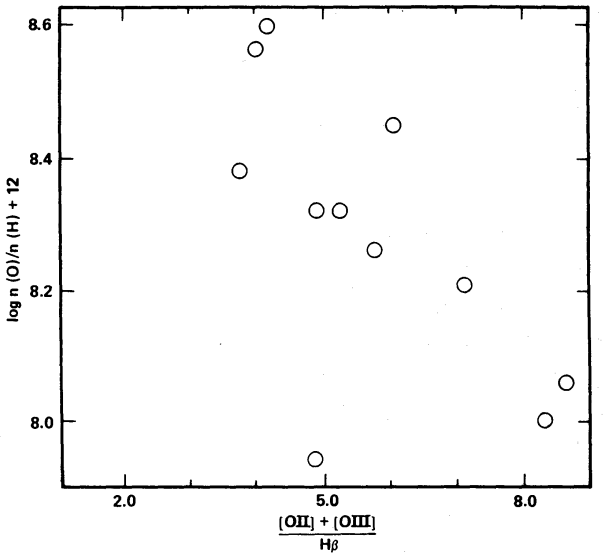

Figure 10. The relationship between $\log N(O)/N(H) + 12$ and ([O II] + [O III])/Hβ. Here [O II] + (O III] denotes the sum of the intensities of 3727, 4959 and 5007. Note the steady decline of $\log N(O)/N(H)$ as [O II] + [O III] increases (*cf.* Fig. 7 of Pagel *et al.* 1979). The discordant point applies to IC131 if we take T_e = 11 500 K; if we assume that $I(4363)$ is too strong, and adopt T_e = 10 000 K, the discordance is removed.

gradient, Δ, in [log O/H] is 0.13 per kpc. The points of highest weight are those where electron temperatures are fixed by the (4959 + 5007)/4363 ratio. In some nebulosities, the 3727/7325 line ratio is helpful although it cannot give as accurate a value as can the [O III] data, partly because this ratio depends on electron density as well as temperature. For four nebulosities *ad hoc* temperatures were assigned, primarily on basis of evidence from work of Shields & Searle (1978) on M101, by Alloin *et al.* (1979) and by Pagel *et al.* (1979). The gradient can be steepened if one assumes that the temperatures in the interior regions are even lower. A plot of $\log N(O)/N(H)$ versus ([O II] + [O III])/Hβ (Fig. 10) shows a tendency for a decline with distance. Again, IC131 appears to be discordant. A plot of $N(N)/N(H)$ shows the same features as the $N(O)/N(H)$ plot – a steady decrease in the nitrogen abundance with distance from the nucleus. A plot of log O/N against r shows a scatter within ±0.14 about a mean value +1.25. A plot of $\log N(Ar)/N(H)$ shows a decrease with r while $\log N(O)/N(Ar)$ indicates no dependence on distance and a scatter within ±0.16 about a value of 2.4. Plots of $\log N(O)/N(S)$ or $\log N(N)/N(S)$ show a large scatter with no trend depending on distance. We conclude that scatter arises largely from uncertainties in the ICF and lack of observations of the nebular transition in [S III]. The mean O/S ratio appears to be about 36.

Pagel & Edmunds (1981) have noted that the dependence of the N/H and O/H ratios on distance as found by Dopita *et al.* (1980) from supernova remnants are in good accord with the H II region data (Pagel *et al.* 1979).

Although the $N(\text{element})/N(H)$ ratio declines with r for all elements except He, the $N(\text{element})/N(O)$ ratio seems to remain fairly constant. In Table 6, we compare the logarithm of the $N(\text{element})/N(O)$ ratio observed in M33 with those found in the Orion nebula, in the Sun, in planetaries and in the Large and Small Magellanic Clouds.

Within a factor of about 2, the Orion Nebula and M33 have similar abundance ratios with respect to hydrogen. The solar values for Ar and Cl are uncertain but an argument can be made that the $N(Cl)/N(O)$ and $N(Ar)/N(O)$ ratios do not vary by more than a factor of 2 or

Table 6. Comparison of elemental abundance ratios in M33 with respect to oxygen.

	log N(el)/N(O)					
	M33	Orion	Sun	Planetary nebulae	LMC	SMC
N	−1.25	−0.99	−0.9	−0.69	−1.41	−1.55
Ne	−0.77	−0.85	−0.82	−0.66	−0.66	−0.62
S	−1.55	−1.34	−1.6	−1.53	−1.53	−1.81
Cl	−3.56	−3.60	−3.34	−3.40	−3.5	−3.5
Ar	−2.40	−2.05	−2.30	−2.28	−2.08	−2.24

Sources of data are as follows:

Orion Nebula: Peimbert & Torres-Peimbert (1977).
Sun: Ross & Aller (1976) updated for new determinations of C, N and O abundances by Lambert (1978) and sulphur abundance by Lambert & Luck (1978).
Planetaries: Aller (1978) except for new sulphur data by Dinerstein (1980) and by Beck *et al.* (1981).
Magellanic Clouds: values quoted are from a model analysis (Aller *et al.* 1979), except for Cl which is taken from Pagel *et al.* (1978). The derived compositions were in good agreement with those found by Pagel *et al.* (1978) where comparisons could be made, and in harmony with results by Peimbert & Torres-Peimbert (1974, 1976), Dufour (1975) and Dufour & Harlow (1977).

3 from one type of object to another. The planetary nebulae compilation includes objects that show an enrichment of nitrogen; the mean value reflects this effect. In the Magellanic Clouds, all authors have agreed that not only is nitrogen depleted with respect to hydrogen, but also with respect to oxygen if one uses the Sun or the Orion nebula as a standard.

Thus it would seem as though the relative rate of manufacture of oxygen and heavier elements proceed at not greatly dissimilar rates in M33, our Galaxy and the Magellanic Clouds. The absolute rate apparently does not change from point to point in the Magellanic Clouds. None of the aforementioned observing teams have found any dependence of chemical composition on position in these objects. Yet in spiral galaxies such as M33, M101 (Smith 1975; Hawley 1978; Shields & Searle 1978), or in NGC 300 (Pagel *et al.* 1979) there is a strong O/H gradient, although probably no N/O gradient. Although variations in excitation effects (such as temperature of the illuminating star) and dust may play some role as noted by Searle (1971), there appears to be no doubt as to the reality of an actual abundance gradient (see, e.g. Collin-Souffrin & Joly 1976).

A number of hypotheses have been proposed to account for the varying ratios of N/O and the origin of nitrogen. It appears to be of mostly primary rather than secondary origin. A large number of free parameters are available – the rate of star formation, the initial mass function for the stars, the gas density, and the fraction of the total mass which is in the form of gas. Various theoretical scenarios can be devised. Edmunds & Pagel (1978) suggested that nitrogen is contributed primarily by low-mass stars and that in the past differing rates of star formation may have occurred. Stars of intermediate mass ($4-10M_{\odot}$) may also play an important role. Plausible scenarios have been proposed by a number of investigators, e.g. Alloin *et al.* (1979). Formation of C, N and O depends on the gas mass fraction of the galaxy and the initial mass function. The rate of star formation affects the nitrogen abundance, in the sense that the greater the rate early in the history of a galaxy, the greater will be the resultant nitrogen abundance (for a fixed gas fraction). They interpret the nitrogen deficiency in M33 as suggesting that the initial mass function may have been flatter, i.e.

with more very massive stars that make oxygen. There were relatively fewer stars of intermediate mass that make N. The yield is then adjusted by increasing the proportions of stars below solar mass.

The ambiguities appear to be still so large that any unique history of element building would be difficult to establish. Dopita *et al.* (1980) conclude that no galactic enrichment theory is successful in explaining their observations of M33. Although nitrogen is produced as a primary product of nuclear reactions, later – at a stage when the ratio of gas/star mass had declined – it is produced as a secondary element.

Information on heavier elements such as argon and sulphur which must come from more massive stars might give us additional constraints that would help in narrowing the range of plausible scenarios.

Acknowledgments

We are grateful to the staff of Lick Observatory who contributed so much to the success of the observational programme. We are deeply indebted to our associates, Professors Holland Ford and Harland Epps who helped us secure some of the observations at the telescope. George Jacoby and Mrs Zdenka Plavcova supplied valuable computer programs as did also C. D. Keyes, who devised the theoretical modelling program and performed many other services. Professor B. E. J. Pagel read the manuscript and made many valuable suggestions. We acknowledge with thanks services rendered by the Office of Academic Computing. This programme was supported in part by National Science Foundation Grant AST 77-21-22 to the University of California, Los Angeles.

References

Aller, L. H., 1942. *Astrophys. J.*, **95**, 52.
Aller, L. H., 1950. *Astr. J.*, **56**, 34.
Aller, L. H., 1954. *Astrophysics II*, facing p. 232, Ronald Press, New York.
Aller, L. H., 1956. *Gaseous Nebulae*, Wiley, New York.
Aller, L. H., 1978. *Proc. astr. Soc. Aust.*, **3**, 213.
Aller, L. H., Walker, M. F. & Czyzak, S. J., 1968. *Astrophys. J.*, **151**, 491.
Aller, L. H., Keyes, C. D. & Czyzak, S. J., 1979. *Proc. Natn. Acad. Sci. USA*, **76**, 1525.
Aller, L. H., Keyes, C. D., Ross, J. E., & Czyzak, S. J., 1980. *Astrophys. Space Sci.*, **67**, 349.
Alloin, D., Collin-Souffrin, S., Joly, M. & Vigroux, L., 1979. *Astr. Astrophys.*, **78**, 200.
Balick, B., 1975. *Astrophys. J.*, **201**, 705.
Balick, B. & Sneden, C., 1976. *Astrophys. J.*, **208**, 336.
Beck, S. C., Lacy, J. H., Townes, C. H., Aller, L. H., Geballe, T. R. & Baas, F., 1981. *Astrophys. J.*, in press.
Benvenuti, P., D'Odorico, S. & Peimbert, M., 1973. *Astr. Astrophys.*, **28**, 447.
Boulesteix, J., Courtes, G., Laval, A., Monnet, G. & Petit, H., 1974. *Astr. Astrophys.*, **37**, 33.
Brocklehurst, M., 1971. *Mon. Not. R. astr. Soc.*, **153**, 471.
Butler, S. E., Bender, C. T. & Dalgarno, A., 1979. *Astrophys. J.*, **230**, L59.
Churchwell, E., Smith, L. F., Mathis, J., Mezger, P. G. & Huchtmeier, W., 1978. *Astr. Astrophys.*, **70**, 719.
Clarke, W., 1965. *Thesis*, UCLA, quoted in *Stars and Stellar Systems*, eds Middlehurst, B. & Aller, L. H., **7**, 506, 1968, University of Chicago Press, Chicago.
Collin-Souffrin, S. & Joly, M., 1976. *Astr. Astrophys.*, **53**, 213.
Comte, G., 1975. *Astr. Astrophys.*, **39**, 197.
Comte, G. & Monnet, G., 1974. *Astr. Astrophys.*, **33**, 161.
Courtes, G. & Cruvellier, P., 1965. *Ann. Astrophys.*, **28**, 683.
Danziger, I. J., Murdin, P. G., Clark, D. H. & D'Odorico, S., 1979. *Mon. Not. R. astr. Soc.*, **186**, 555.
de Vaucouleurs, G., 1978. *Astrophys. J.*, **223**, 735.
de Vaucouleurs, G. & de Vaucouleurs, A., 1964. *Reference Catalogue of Bright Galaxies*, Texas University Press.
Dinerstein, H., 1980. *Astrophys. J.*, **237**, 486.

Dopita, M., D'Odorico, S. & Benvenuti, P., 1980. *Astrophys. J.*, **236**, 628.
Dufour, R. S., 1975. *Astrophys. J.*, **195**, 315.
Dufour, R. J. & Harlow, W. V., 1977. *Astrophys. J.*, **216**, 706.
Edmunds, M. G. & Pagel, B. E. J., 1978. *Mon. Not. R. astr. Soc.*, **185**, 77P.
Garstang, R. H., 1968. *IAU Symp. No. 34, Planetary Nebulae*, p. 143, eds Osterbrock, D. E. & O'Dell, C. R., Reidel, Dordrecht.
Gordon, K. J., 1969. *Q. Jl R. astr. Soc.*, **10**, 293.
Haro, G., 1950. *Astr. J.*, **55**, 66.
Hawley, S. A., 1978. *Astrophys. J.*, **224**, 417.
Hawley, S. A. & Grandi, S. A., 1977. *Astrophys. J.*, **217**, 420.
Hawley, S. A. & Grandi, S. A., 1978. *Publs astr. Soc. Pacif.*, **90**, 125.
Hodge, P., 1969. *Astrophys. J. Suppl.*, **18**, 73.
Hubble, E. P., 1936. *Realm of the Nebulae*, Yale University Press, New Haven, USA.
Israel, R. P. & van der Kruit, P. C., 1974. *Astr. Astrophys.*, **32**, 363.
Keyes, C. D. & Aller, L. H., 1978. *Astrophys. Space Sci.*, **59**, 91.
Krueger, T. K. & Czyzak, S. J., 1970. *Proc. R. Soc.*, **A318**, 531.
Kurucz, R. L., 1979. *Astrophys. J. Suppl.*, **40**, 1.
Lambert, D. L., 1978. *Mon. Not. R. astr. Soc.*, **183**, 179.
Lambert, D. L. & Luck, R. E., 1978. *Mon. Not. R. astr. Soc.*, **183**, 79.
Lohmann, W., 1974. *Astrophys. Space Sci.*, **29**, 61.
Mathis, J., 1962. *Astrophys. J.*, **136**, 374.
Mathis, J., 1970. *Astrophys. J.*, **159**, 163.
Mayall, N. U. & Aller, L. H., 1939. *Publs astr. Soc. Pacif.*, **51**, 112.
Mayall, N. U. & Aller, L. H., 1942. *Astrophys. J.*, **95**, 5.
Menzel, D. H. & Aller, L. H., 1941. *Astrophys. J.*, **94**, 30.
Mezger, P. G., 1970. *IAU Symp. No. 38*, p. 107, eds Becker, W. & Contopoulos, G., Reidel, Dordrecht.
Mezger, P. G., Pankonin, V., Schmid-Burkg, J., Thum, C. & Wink, J., 1979. *Astr. Astrophys.*, **80**, L3.
Nussbaumer, H., 1971. *Astrophys. J.*, **166**, 411.
Osterbrock, D. E., 1974. *Astrophysics of Gaseous Nebulae*, Freeman, San Francisco.
Pagel, B. E. J. & Edmunds, M. G., 1981. *A. Rev. Astr. Astrophys.*, in press.
Pagel, B. E. J., Edmunds, M. G., Fosbury, R. A. E. & Webster, B. L., 1978. *Mon. Not. R. astr. Soc.*, **184**, 569.
Pagel, B. E. J., Edmunds, M. G., Blackwell, D. E., Chun, M. S. & Smith, G., 1979. *Mon. Not. R. astr. Soc.*, **189**, 95.
Peimbert, M., 1971. *Boln. Obs. Tonanzintla Tacubaya*, **6**, 97.
Peimbert, M., 1970. *Publs astr. Soc. Pacif.*, **82**, 636.
Peimbert, M. & Costero, R., 1969. *Boln. Obs. Tonanzintla Tacubaya*, **5**, 3.
Peimbert, M., Rodriguez, L. & Torres-Peimbert, S., 1974. *Rev. Mex. Astr. Astrofis.*, **1**, 129.
Peimbert, M. & Spinrad, H., 1970. *Astrophys. J.*, **159**, 809.
Peimbert, M. & Torres-Peimbert, S., 1974. *Astrophys. J.*, **193**, 327.
Peimbert, M. & Torres-Peimbert, S., 1976. *Astrophys. J.*, **203**, 531.
Peimbert, M. & Torres-Peimbert, S., 1977. *Mon. Not. R. astr. Soc.*, **179**, 217.
Pradhan, A. K., 1978. *Mon. Not. R. astr. Soc.*, **184**, 89P.
Robinson, L. & Wampler, E. J., 1972. *Publs. astr. Soc. Pacif.*, **84**, 161.
Ross, J. E. & Aller, L. H., 1976. *Science*, **191**, 1223.
Rubin, V. C. & Ford, W. K., 1971. *Astrophys. J.*, **170**, 25.
Sandage, A., 1962. *IAU Symp. No. 15, Problems of Extragalactic Research*, p. 354, ed. McVittie, G., MacMillan, New York.
Sarazin, C. L., 1976. *Astrophys. J.*, **208**, 323.
Searle, L., 1971. *Astrophys. J.*, **168**, 327.
Seaton, M. J., 1975. *Mon. Not. R. astr. Soc.*, **170**, 476.
Shajn, G. A., 1954. *Izv. Krymsk. Astrofis. Obs.*, **2**, 3.
Shields, G. & Searle, L., 1978. *Astrophys. J.*, **222**, 321.
Smith, H. E., 1975. *Astrophys. J.*, **199**, 591.
Stasinka, G., 1978. *Astr. Astrophys. Suppl.*, **32**, 429.
Stasinka, G., 1979. *Astr. Astrophys. Suppl.*, in press.
Stone, R., 1974. *Astrophys. J.*, **193**, 135.
van den Bergh, S., 1960. *Astrophys. J.*, **131**, 215.
van den Bergh, S., 1976. *Astrophys. J.*, **203**, 764.

van der Kruit, P. C., 1973. *Astr. Astrophys.*, **29**, 231.
Walker, M. F., 1964. *Astr. J.*, **69**, 744.
Warner, J. W., 1973. *Astrophys. J.*, **186**, 21.
Warner, P. J., Wright, M. C. H. & Baldwin, J. E., 1973. *Mon. Not. R. astr. Soc.*, **163**, 16.
Whitford, A. E., 1958. *Astr. J.*, **63**, 201.
Wilson, T. L., 1979. *Astr. Astrophys.*, **77**, L3.
Wray, J. E. & Corso, G. J., 1972. *Astrophys. J.*, **172**, 577.
Wright, M. C. H., Warner, P. J. & Baldwin, J. E., 1972. *Mon. Not. R. astr. Soc.*, **155**, 337.
Wright, M., 1971. *Astrophys. Lett.*, **7**, 209.

Appendix: notes to Tables 2, 3 and 5 – data for individual nebulosities

MA11. This low excitation nebulosity appears to be illuminated by stars which do not have a strong ultraviolet radiation field. If Kurucz models are used, $T_e < 37\,500$ K. For reasons presented in the text we take $T_e = 8000$ K. Arguments can be presented in favour of an even lower value. No reliable measurement of λ 4363 could be made.

IC142. From rf measurements, Israel & van der Kruit (1974) find a total mass of $125\,000 M_\odot$. The observed ionization requires five O5 stars or 17 O6 stars. We adopted $T_e = 8000$ on the basis of theoretical models and absence of λ 7325 [O II]. The derived extinction $C(\mathrm{H}\beta) = 0.70$ is to be compared with rf values of $C = 1.2$ and 2.2 and an optical estimate of 0.08 (Israel & van der Kruit 1974). They obtain a mass of $1.2 \times 10^5 M_\odot$.

NGC595. This is one of the 'supergiant' H II regions with an ionized gas mass of the order of $10^6 M_\odot$ (Israel & van der Kruit 1874). They find it to be material bounded with a dense core and a faint extended component 1.7 × 1 arcmin. Observed with similar low resolution the giant galactic source W51 also shows a core–halo structure. Our measured intensities are in fairly good agreement with those of Smith (1975). Comte & Monnet (1974) obtained [N II] and [S II] intensities lower than those we have found. We adopted $T_e = 9000$ K which is suggested by the 3727/7325 ratio, but which may be a trifle high.

MA2. This is a medium excitation object. We adopted $T_e = 8000$ K. No [O II] λ 7323 data are available.

MA3. From the 6717/6730, (4959 + 5007/4363, and 3727/7325 ratios we adopted $T_e = 9300$ K and $\log x = -1.70$. From [Cl III] we obtain $n(\mathrm{Cl}^{2+})/n(\mathrm{H}^+) = 1.05 \times 10^{-7}$ and then with the aid of model interpolation we find $\log n(\mathrm{Cl}) + 12 = 5.02$.

NGC604. This bright nebulosity appears to be comparable with 30 Doradus, although Wright (1971) finds it to be dynamically unstable. Israel & van der Kruit (1974) suggest a dense core with a diameter of about 43 pc and a surrounding halo of 2.3 × 1.2 arcmin. The neutral component is approximately $5 \times 10^6 M_\odot$ and the ionized gas is about $1.6 \times 10^6 M_\odot$ requiring the equivalent of 33 O5 stars or 113 O6 stars to produce the ionization. This bright nebulosity has been the subject of many recent investigations: Mathis (1962), Aller, Walker & Czyzak (1968), Peimbert & Spinrad (1970), Peimbert (1970), Smith (1975), Hawley & Grandi (1977) and Dopita *et al.* (1980). Our measured intensities agree fairly well with those of Smith, although there appear to be some differences with Hawley & Grandi who observed the integrated light of the nebulosity. From the 3726/3729 [O II] ratio, Aller *et al.* found $N_e = 70$–100 cm^{-3}, while Israel & van der Kruit got $N_e = 47$ cm^{-3}. With our present data, diagnostics are: $I(5007 + 4959)/I(4363) \rightarrow T_e = 10\,800$ K [O III]; $6584/5755 \rightarrow T_e = 8900$

[N II] (assuming $N_e = 100$); 3727/7325 → $T_e = 9000$ K ($N_e = 100$) [O II]. Hence we have used $T_e = 10\,800$ for O^{2+}, Ne^{2+}, Ar^{2+} and Cl^{2+}, and $T_e = 8900$ for O^+, N^+, S^+ and S^{2+} in calculating ionic concentrations. We find $n(Cl^{2+})/n(H^+) = 5.13 \times 10^{-7}$ and estimate a total chlorine abundance of 5.7×10^{-7}. For nitrogen and sulphur, both our ionic and total abundances are smaller than those found by Hawley & Grandi, who get $\log n(N) = 7.23$ and $\log n(S) = 7.28$; hence N/S = 0.89.

The differences between Hawley & Grandi's results and ours arise almost entirely from differences in the measured intensities. They used an aperture of 14 arcsec; we employed a 2 × 2 arcsec slot at a fixed point near an edge of the bright part of the nebulosity:

	λ 6312	λ 6584	λ 6717	λ 6730
14 arcsec aperture (H & G)	4.0	41	11.3	15
2 × 2 arcsec slot (K & A)	0.98	28	10.8	10

(See Figs 6 and 7).

IC131. From the (4959 + 5007)/4363 ratio we get $T_e = 11\,500$ K, while the 6717/6730 ratio indicates, $N_e \leqslant 100$ cm^{-3}. Unfortunately, the 4363 intensity is suspect. With $T_e = 11\,500$ K, the abundances of nitrogen, oxygen and neon appear to be abnormally low compared with other nebulosities at the same distance from the nucleus and from ([O II] + [O III])/Hβ (compare Pagel *et al.* 1979). If we select $T_e = 10\,000$ K much more plausible values of the abundances are obtained. We find $C(H\beta) = 0.47$, which is close to the mean of two estimates by Israel & van der Kruit.

MA9a. We chose $t = 1.0$ for the analysis of this nebulosity which is characterized by moderate excitation. The [S II] ratio suggests $N_e \sim 200$. The ICF for neon is uncertain.

IC133. We carried out calculations for both $T_e = 11\,000$ and $10\,000$ K, which are values consistent (within the observational errors) with the 3727/7325 and 6717/6730 ratios for $N_e = 30$ and 100, respectively. The nebular excitation is moderately high.

NGC588. Our measured line intensities are in good agreement with those of Smith. The oxygen and other abundances are low. We find $T_e = 12\,800$ K and $N_e \sim 350$ cm^{-3} but $I(4363)$ may have been estimated too strong by a factor of about 1.5. Israel & van der Kruit (1974) find a total mass of $195\,000\,M_\odot$ for the region and suggest that three O5 or 11 equivalent O6 stars would be required to produce the observed ionization.

IC132. This object has fairly high excitation for which Israel & van der Kruit (1974) find a mass of $140\,000\,M_\odot$. T_e and $\log x$ appear to be well determined from $N_1 + N_2/4363$ and 6717/6730, respectively, as 12 300 K and −1.65. The intensities appear to be in good agreement with measurements by Smith (1975), although we find a lower electron temperature. The abundances of O, Ne and N are lower than found in the interior regions of M33.

MA1. Is a very faint nebulosity for which our data are very limited.